REVIEW OF LITERATURE

The global warming and terrestrial ecosystem

Atmospheric CO_2 is the most important of the radiative forcing components driving the ongoing change in climate(IPCC, 2007). The global increases in atmospheric CO_2 concentration are driven primarily by CO_2 release during fossil fuel combustion and land use change. On average, 40% of the CO_2 released by fossil fuel combustion stays in the atmosphere and the remainder is removed from the atmosphere by Earth's oceanic and terrestrial biosphere. Life on Earth, on land and in the oceans, offsets the impact of human modification of the global carbon cycle. Quantifying and projecting the removal of atmospheric CO_2 is critical to understanding how the Earth's climate will change and evolve over the next years, decades, and centuries. The Fourth Assessment Report (AR4) of Working Group 1 of the Intergovernmental Panel on Climate Change (IPCC, 2007) was the first to address the "Earth System" by including a coupled carbon cycle and climate.

Here are a few facts excerpted from the recent Fourth Assessment Report to help frame the importance of the global carbon cycle and the rise in atmospheric CO_2 concentration (from frequently asked question 7.1, IPCC, 2007): "*The concentration of carbon dioxide is now 379 parts per million, very likely (>90% probability) much higher than any time at least 650 thousand years, during which atmospheric carbon dioxide remained between 180 and 330 parts per million. The current rate of increase in atmospheric carbon dioxide is very likely at least seven times faster than*

at any time during the two thousand years before the Industrial Era. Finally, the recent rate of change is dramatic and unprecedented; increases in atmospheric carbon dioxide never exceeded 30 ppm in 1000 years- yet now atmospheric carbon dioxide concentrations have risen by 30 ppm in the last 17 years."

The rise in atmospheric CO_2 concentration is driven by emissions of CO_2 from fossil fuel combustion and cement manufacturing is responsible for more than 75% of the increase in atmospheric CO_2 concentration. The remainder of the increase comes from land-use changes dominated by deforestation and associated biomass burning with contributions from changing agricultural practices. All these processes are caused by human activity. The most important consequence of this rise in atmospheric CO_2 concentration is warming the surface temperature of the Earth. Global mean surface temperatures have risen by 0.74 ± 0.18 °C over the last 100 years (1906-2005). Observed warming over several decades has been linked to changes in the large-scale hydrological cycle such as: increasing atmospheric water vapor content; changing precipitation patterns, intensity and extremes; reduced snow cover and widespread melting of ice; and changes in soil moisture and runoff (IPCC, 2007). The resultant global warming and climate change exert increasingly the researchers around the world have begun experiments to investigate the effect of these changes on terrestrial ecosystem (Cao and Woodward, 1998a; Cao and Woodward, 1998b; Kennedy, 1995; e.g. Shaver *et al.*, 2000; Shimizu *et al.*, 2005)

Net ecosystem carbon exchange (*NEE*)

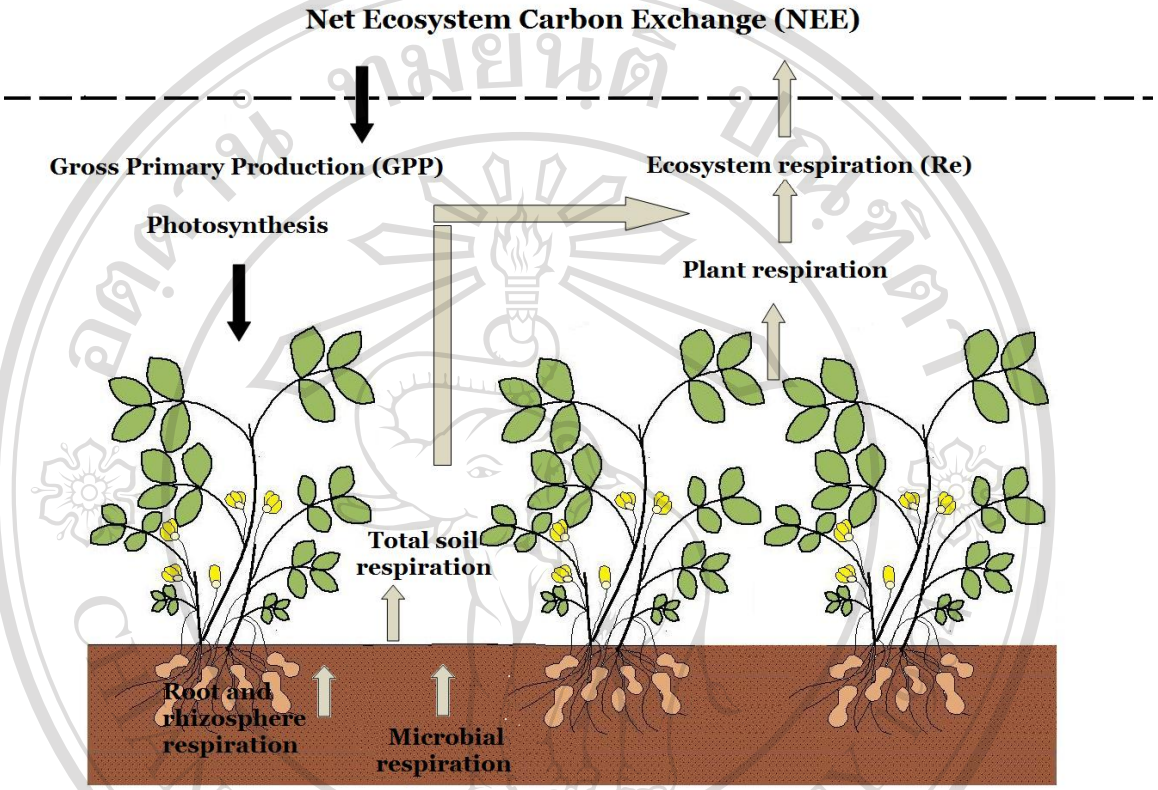

Figure 1.1 Overview of the CO_2 fluxes resulting in net ecosystem exchange *NEE*.

Definitions

Net CO_2 flux density of an ecosystem (net ecosystem carbon exchange: *NEE*) relies on the balance between CO_2 uptake through plant photosynthesis (gross primary production: *GPP*) and CO_2 emission through plant and soil respiration which refers to ecosystem respiration (R_e). A negative value of *NEE* means a net carbon gain by the ecosystem, i.e., a positive net ecosystem productivity (*NEP*), as it may be assumed *NEP* to equal *–NEE*. Theses two terms are used somewhat interchangeably, with *NEE* used more often to refer to these fluxes when they are addressed from a

measurement of gas exchange rates using atmospheric measurements over time scales of hours, whereas *NEP* is more often used to refer to the same processes if measurements are based on ecosystem-carbon stock changes, typically measured over a minimal period of one year. The definitions are summarized in Equation 1.1 and Figure 1.1

$$-NEP = NEE = GPP - R_e, \quad (1.1)$$

Controlling factors

Photosynthetically active radiation (*PAR*) is the main climatic variable that drives plant photosynthetic processes (Larcher, 2003). Several studies show an increase of CO_2 uptake under cloudy condition (Goulden *et al.*, 1997; Suyker *et al.*, 2004; Urban *et al.*, 2007). These conditions, notably high clouds, more diffuse radiation, which penetrates deeper into the canopy, is available for photosynthesis. In addition to *PAR*, air and soil temperature (T_a, T_s), water vapor deficit (*VPD*) and soil water availability (e.g., soil water content; *SWC*) affect the assimilation rate (Larcher, 2003). Previous studies have indicated that *NEE* is strongly influenced by water status, including the effects of water stress on stomatal conductance, and the influence of moisture on heterotrophic and autotrophic respiration (Fu *et al.*, 2006; Kim and Verma, 1990; Li *et al.*, 2005; Nakano *et al.*, 2008; Sims and Bradford, 2001). Fu *et al.* (2006) and Sims and Bradford (2001) found an afternoon depression in *NEE* during midsummer in a semi-arid steppe in Inner Mongolia and in a mixed-grass prairie in the United States, respectively. Sims and Bradford (2001) suggested that this *NEE* reduction probably resulted from stomatal closure in leaf tissue due to high *VPD*, In

addition to the stomatal limitation, Fu *et al.* (2006) inferred that high temperature at midday caused the *NEE* reduction through a decrease of photosynthesis and an increase of R_e. Li *et al.* (2005) and Kim and Verma (1990) illustrated *NEE-PAR* curves grouped by values of soil moisture and *VPD*, which demonstrated that *NEE* was reduced when soil moisture was low or the *VPD* was high. They suggested that a soil water deficit might aggravate *VPD*-induced decrease in carbon uptake, which as consistent with a study by Nakano *et al.* (2008).

As mentioned above, the *NEE* is determined also by the ecosystem respiration, which consists of plant and soil respiration. A wide range of studies has shown that R_e is positively correlated with temperature. Moreover it depends on soil moisture, which under drought conditions can have a substantial influence and mask the temperature response (e.g. Davidson *et al.*, 2000; Gaumont-Guay *et al.*, 2006; Jarvis *et al.*, 2007; Reichstein *et al.*, 2002a; Reichstein *et al.*, 2002b; Xu *et al.*, 2004). There is mounting evidence that the temperature sensitivity of respiration (Q_{10}) declines with increasing temperature and decreasing soil moisture (Curiel Yuste *et al.*, 2003; Reichstein *et al.*, 2002a; Reichstein *et al.*, 2002b; Xu and Baldocchi, 2004; Xu and Qi, 2001). Hence, in systems without water limitation R_e is generally determined by temperature (Griffis *et al.*, 2004; Huxman *et al.*, 2003). Ecosystem respiration rates are also positively correlated with photosynthesis rates or site productivity, illustrating some important biotic controls on respiration (Craine *et al.*, 1999; Janssens *et al.*, 2001). The correlation between respiration and photosynthesis rates presumably reflects the role of available carbon substrates in affecting plant and soil microbe respiration.

Drought stress effect on peanut growth

In many parts of the world, peanut is grown in rainfed conditions. Peanut is frequently subject to drought stresses of different duration and intensities during some period of the growing season (Dwivedi *et al.*, 1996). Drought stress has an adverse influence on water relations (Babu and Rao, 1983), photosynthesis (Bhagsari *et al.*, 1976), and growth and yield of peanut. Several researchers have found that peanut sensitivity to water deficit depend on the stage of growth.

Rate of transpiration, leaf temperature and canopy temperature are important parameters that influence water relations in peanut. Leaf and canopy temperature of irrigated plants is generally equal to or less than ambient air temperature but rainfed plants often have a higher canopy temperature than ambient air temperature. Transpiration rate generally correlates with incident solar radiation under sufficient water availability. However, drought-stressed plants transpire less than unstressed plants (Reddy et al., 2003). The pre-flowing phase is less sensitive to water stress than the flowering phase. Yield reductions are greatest with stress imposed during the period between pegging and pod development and lowest with stress imposed from pod development to maturation (Reddy et al., 2003).

The mean optimal air temperature range for vegetation growth of peanut is between 25 and 30 °C, which is warmer than the optimum range for reproductive growth, which is between 22 and 24 °C (Cox, 1979). Short or long-term exposure to air and soil temperature above the optimum range can significant reduces peanut yields (Golombex and Johansen, 1997). Increasing daytime temperature from 26-30 °C to 34-36 °C significantly reduced the number of subterranean pegs, pod and seed size, and reduced seed yield by 30-35% (Cox, 1979). Prasad *et al.* (2000) investigated

the effects of daytime soil and air temperature of 28 and 38 °C, from the start of flowering until maturity, and reported 50% reduction in pod yield at high temperature.

Relative water content, leaf water potential, stomatal conductance, rate of transpiration, leaf temperature and canopy temperature are important parameters that influence water relations in peanut. Relative water content of leaves is higher in the initial stages of leaf development and declines as the dry matter accumulates and leaf matures (Jain *et al.*, 1997). Babu and Rao (1983) found that relative water content of droughted plants more than twice lower than non-stressed plants. Leaf water potential of peanut leaves show large diurnal variation with high values in the morning when solar radiation and vapor pressure deficit are low, followed by low values around midday and gradually rises after midday (Erickson and JKetring, 1985). Osmotic potential follows the same pattern but ranges less widely than leaf water potential. Leaf and canopy temperature of irrigated plants are generally equal to or less than ambient air temperature but rainfed plants often have a higher canopy temperature than ambient air temperature. Transpiration rate generally correlates to the incident solar radiation when sufficient water is available for plants. However, droughted plants transpire less than unstressed plants. The same pattern was observed for stomatal conductance (Mohandas *et al.*, 1989).

Black *et al.* (1985) recorded lower leaf water potent potential, turgor potential and stomatal conductance when moisture stress was imposed, however, stomatal conductance was more strongly affected than leaf water status. Stomatal conductance was poorly correlated with leaf water potential and soil water potential. The conservative influence of decreased stomatal conductance in non-irrigated plants was negated by increases in leaf-to-air vapor pressure difference caused by associated

higher leaf temperatures (Craufurad *et al.*, 2000). Transpiration rates were therefore, similar in both treatments and the lower total water use of non-irrigated stand resulted entirely from its smaller leaf area index. Subramaniam and Maheswari (1990) reported that leaf water potential, transpiration rate and photosynthetic rate decreased progressively with increasing duration of water stress indicating that plants under mild stress were postponing tissue dehydration. Stomatal conductance decreased almost steadily during the stress period indicating that stomatal conductance was more sensitive than transpiration during the initial stress period.

Canopy photosynthesis is reduced by moisture stress due to reduced stomatal conductance and reductions in leaf area. As an accumulation deficit in soil water increase, stomata start closing as a mechanism to reduce transpiration. As a consequence, the entry of carbon dioxide exchange is also reduced. The decrease in conductance of mesophyll cells due to moisture stress results in low conductance of carbon dioxide and a reduction in photosynthesis. Bhagsari *et al.* (1976) observed large reductions in photosynthesis and stomatal conductance as the relative water content of peanut leaves decreased from 80 to 70%. The main effect of a soil water deficit on leaf carbon exchange rate is exerted through stomatal closure. Bhagsari *et al.* (1976) reported reduced carbon exchange rate, decreased transpiration and increased stomatal resistance with in 3 days of withholding water in potted pants. Under field conditions, Allen *et al.* (1976) found reduced stomatal resistance by 7 days after stress and significant differences within ten days between stressed and non-stressed plants. The long-term effect of soil water deficit on canopy assimilation is a reduction in leaf area. Soil water deficit induces a reduction in leaf area expansion, by temporary leaf wilting or rolling, by reducing the supply of carbohydrates, and by

early leaf senescence (Clifford et al., 1993; Collino et al., 2001; Reddy et al., 2003). The consequent reduction in leaf area determines a decrease in the crop's ability to capture light resources, resulting in a negative influence on both crop productivity and dry matter production.

Eddy-covariance method

The eddy-covariance method provides a direct measure of net CO_2 exchange across the canopy-atmosphere interface (Baldocchi, 2003; Foken and Wichura, 1996). This task is accomplished by using micrometeorological theory to interpret measurements of the covariance between vertical wind velocity and scalar atmospheric data series, and yields values of fluxes of these properties (Baldocchi *et al.*, 1988). Such flux measurements are widely used to estimate momentum, heat, water, and carbon dioxide exchange, as well as exchange of methane and other trace gases. With current technology, the eddy-covariance method is able to measure net CO_2 exchange over short and long times scales (hour, days, seasons, and years) (Baldocchi *et al.*, 2001; Wofsy *et al.*, 1993). Another attribute of the eddy-covariance method is its ability to sample a relatively large area of land. Tropical footprints have longitudinal length scales of a hundred meters to several kilometers (Schmid, 1994).

Turbulence is characterized by disordered, eddying fluid motions over a wide range of length scales. Turbulence productions or turbulent flows, induced by shear stress and buoyancy, consist of many different size turbulence elements, the eddies. They act as "means of conveyance" for physical properties such as momentum or CO_2. Thus, the vertical flux density at a given point in space can be determined as the product of the vertical wind component and the property of interest. As turbulence is

highly variable and chaotic in space and time, it can be treated as a stochastic process. Hence, to get a reliable estimate of the vertical flux density an ensemble average should be calculated. In practice, it is neither possible to make an average over many situations under identical conditions at one given point in a horizontal plane at a given height. Fortunately, the ergodic or "frozen turbulence" hypothesis, which states that time averages measured at a single point are equal to the spatial averages, is assumed to be fulfilled.

Horizontal homogeneity simplifies the determination of vertical flux densities, because advective terms can be ignored. Hence, the statistical characteristics only vary in the vertical. Homogeneity is given if an adequate fetch is present and therefore the flow can be considered as adapted to the surface. If the turbulent characteristics do not vary with time, the time series are statistically stationary. Under this condition, Reynolds decomposition can be applied. The motion of a turbulent fluid, like air, can be defined at any instant in time as being equal to the sum of its mean state (denoted by overbar) and its fluctuation from the mean (denoted by a prime) (Figure 1.2):

$$x(t) = \bar{x} + x'(t). \qquad (1.2)$$

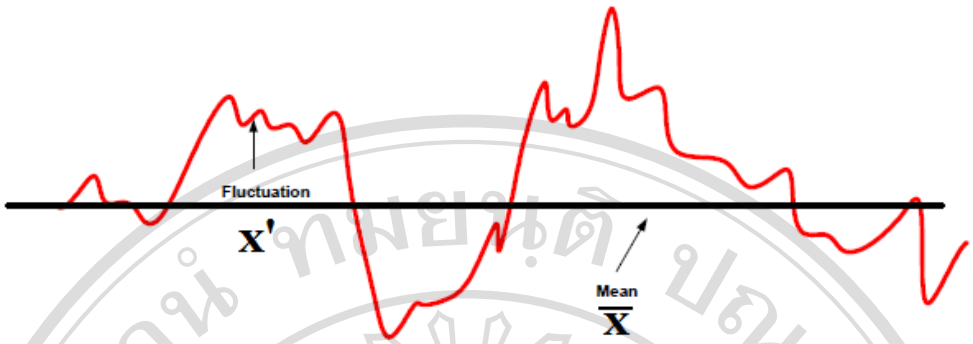

Figure 1.2 Conceptual representation of mean and fluctuation time series of a turbulent quantity like wind velocity, temperature, water vapor or carbon dioxide.

Applying the ergodic hypothesis and the assumption of homogeneity, therefore, the vertical flux density can be calculated as the covariance between the vertical wind component w and a property of interest x:

$$\text{covariance}\,(w,x) = \frac{1}{N}\sum_{i=1}^{N}(w_i - \overline{w})(x_i - \overline{x})\,. \qquad (1.3)$$

Reynolds'Rules of Averaging are used to provide a statistical representation of turbulent wind, its non-Gaussian attributes and turbulent fluxes (Reynolds, 1895). The important properties associated with Reynolds' averaging rules include:

(i) the mean product of two fluctuating variable is a function of the product of the individual means plus a covariance, $\overline{xy} = \overline{x}\,\overline{y} + \overline{x'y'}$;

(ii) the average of any fluctuating component is zero, $\overline{x'} = 0$; and

(iii) the average of the sum of two components is additive, $\overline{x + y} = \overline{x} + \overline{y}$.

Applying these assumptions and assuming that the average vertical wind component equals zero, the vertical flux density F becomes:

$$F = \text{covariance}\,(w,x) = \frac{1}{N}\sum_{i=1}^{N} w_i' x_i' = \overline{w'x'}. \qquad (1.4)$$

Accordingly, the vertical turbulent flux densities of carbon dioxide (F_c), water vapor or latent heat (λE), and sensible heat (H) are calculated as:

$$F_c = \overline{w'c'}, \qquad (1.5)$$

$$\lambda E = \lambda \overline{w'q'}, \qquad (1.6)$$

$$H = \rho_a C_p \overline{w'T_a'}, \qquad (1.7)$$

where c is the CO_2 concentration, λ is the latent heat of vaporization, q is water vapor density, ρ_a is the density of air, C_p is the specific heat of air, and T_a is the air temperature.

Eddy- covariance method in theory

The atmosphere contains turbulent motions of upward and downward moving air that transport trace gases such as CO_2. The eddy-covariance method measures theses turbulent motions to determine the net difference material moving between the canopy and the atmosphere. The factors behind the difference may be studied by investigating the law of conservation of mass (Stull, 1988)

$$\frac{\partial \rho_s}{\partial t} + \frac{\partial u \rho_s}{\partial x} + \frac{\partial v \rho_s}{\partial y} + \frac{\partial w \rho_s}{\partial z} = S + D\,, \qquad (1.8)$$

where ρ_s is the scalar density, *u, v,* and, *w* are the wind velocity components, respectively, in the directions of the mean (*x*), and lateral wind (*y*), and normal to the surface (*z*). *S* is the source/sink term and *D* is the molecular diffusion term. Molecular diffusion is significant only in the molecular sublayer, within the first centimeter of the surface (Stull, 1988). The later gradients and the molecular diffusion will be neglected afterwards. With the case of assessing turbulent transfer CO_2 in the atmosphere, the conservation equation used to deduce the exchange of carbon in and out of the plant-soil system on the basis of eddy-covariance measurements made in the surface boundary layer several meters above a plant canopy. After application of the Reynolds decomposition, the instantaneous values of *u*, *v*, *w* and ρ_s are divided into an average and fluctuation ($u = \overline{u} + u', v = \overline{v} + v', w = \overline{w} + w', \rho_s = \overline{\rho_s} + \rho_s'$ where the overbars characterize time averages and the primes fluctuation around the average), averaging, integration along *z*, and assumption of no horizontal eddy flux divergence, Equation (1.8) becomes:

$$\int_0^{z_m} S dz = \overline{w' \rho_s'}_{z_m} + \int_0^{z_m} \frac{\partial \overline{\rho_s}}{\partial t} dz + \int_0^{z_m} \overline{u} \frac{\partial \overline{\rho_s}}{\partial x} dz + \int_0^{z_m} \overline{w} \frac{\partial \overline{\rho_s}}{\partial z} dz\,, \qquad (1.9)$$

I **II** **III** **IV** **V**

where **I** represents the scalar source/sink term that corresponds to the net ecosystem exchange when the scalar is CO_2 and to the ecosystem evapotranspiration when the scalar is water vapor; **II** represents the eddy flux at height z_m (the flux which is measured by eddy-covariance methods); **III** represents the storage of the scalar below the measurement height; **IV** and **V** represent the fluxes by horizontal and vertical advection of ρ_s, respectively.

Under ideal conditions, the scalar concentrations and wind velocities in the atmosphere are steady with time (term **III** equals zero) and the underlying surface is horizontally homogeneous and on flat terrain (there is no advection, term **IV**). The mean vertical wind speed is tropically small, especially above short vegetation, and it may be assumed that the vertical advection term (**V**) also vanishes. In these conditions, the turbulent flux can be obtained from the eddy-covariance methods at a height z_m to represent the contribution of the integrated sources and sink below the measurement height. In the case of CO_2 fluxes, it defines as the net ecosystem CO_2 exchange (*NEE*) (Aubinet *et al.*, 2000):

$$\overline{w'\rho'_s}_{z=z_m} = \int_0^{z_m} S dz = NEE , \qquad (1.10)$$

where the source term includes the soil respiration.

Eddy-covariance method in practice

The eddy-covariance method is not without weakness. The requirements for the use of this method include a homogeneous flat terrain, steady-state environmental

conditions and that the underlying vegetation extends upwind for an extended distance (Baldocchi, 2003).

Nighttime problems

A major problem in eddy-covariance is the likely underestimation of nighttime respiration fluxes. At night the thermal stratification of the atmosphere is stable or turbulent mixing is weak. Under this condition, CO_2 exiting leaves and the soil may not reach a set of instruments at a reference height above the canopy, causing the eddy-covariance method to underestimate nighttime respiration when compared with scaled up chamber estimates from measurements on soil, foliage and wood tissue. Zamolodchikov *et al.* (2003) found the nocturnal eddy-covariance method to underestimate scaled up chamber estimates in Russian Far East tundra by 30%, similar to the 50% underestimate by Bolstad *et al.* (2004) for northern deciduous forests.

A commonly used approach to limit this nighttime underestimation is to add to the eddy CO_2 flux, a term accounting for the CO_2 storage (**III** in Equation (1.9)) in the layer between the ground and the measurement height. Under the non –steady conditions identified above, the CO_2 storage in the underlying airspace is non-zero, so must be added to the eddy-covariance measurement. To measure the CO_2 storage term accurately, one must measure temporal changes in CO_2 above the canopy and, at least, two heights within the canopy (Baldocchi, 2003). Lee *et al.* (1996) observed the nocturnal CO_2 exchange over a mixed deciduous forest, found that the storage term was significant component of the nocturnal CO_2 exchange when the friction velocity was small. The value CO_2 storage term is greatest around sunrise and sunset when

there is a transition between nocturnal respiration and photosynthesis and between the stable nocturnal boundary layer and day time convective turbulence (Goulden *et al.*, 1996). However, even when the CO_2 storage is taken into account, uncertainty still persists about the accuracy of measurements of nighttime respiration. The observed fluxes may be found to correlate with the wind speed or more exactly with the frictions (u_*), which is a turbulent velocity scale and can be understood as a measure of the turbulence intensity (Stull, 1988). The respiration process itself should not depend on turbulence. It seems probable that there are some additional, non-turbulent, processes removing CO_2 from the air layer below the measurement height either vertically or horizontally.

Insufficient turbulent mixing, incorrect measurement of the storage term of CO_2 in the air space and soil, and the drainage of CO_2 out of the canopy volume at night have been posited as reasons why the eddy-covariance method underestimates CO_2 flux densities at night (Lee, 1998; Lindroth *et al.*, 1998). Alternatively, it is common practice to apply an empirical correction to compensate for the underestimate of nighttime CO_2 flux measurements. Anthoni *et al.* (1999) replace data with a temperature-dependent respiration function that is derived from soil chamber. Other corrections eddy flux measurements under stable condition are based on the rejection of measurements below a certain threshold of friction velocity (u_*), beyond which flux seems to level off and the so-called u_* correction (Falge et al., 2001). Missing data in the series are gap-filled with empirical regression models of respiration response to air or soil temperature, estimated using data collected during well mixed, windy period at night (Falge et al., 2001). However, both the threshold of u_* and respiration models seem to be strictly site dependent.

Coordinate rotation

Streamline are usually not exactly parallel to the underlying surface, but sonic anemometers are rarely exactly aligned with either surface or streamline and will induce a non zero-mean vertical wind component, if the coordinate system is defined along the geopotential field (Wilczak *et al.*, 2001). These disturbances in the *w* values are usually taken into account by rotating the coordinate system to coincide with the local streamline. Traditionally a double rotation, in which the coordinate system is rotated around the *z*-axis ($\overline{v} = 0$) and around the *y*-axis ($\overline{w} = 0$), is performed for every averaging period (e.g., 30-min). Recently, it has been suggested that a more appropriate practice would be the determination of a fixed plane for the site over a longer period (e.g., a few months). In this planar fit method, the mean vertical wind component is thus allowed to have non-zero values during individual 30- or 60-min periods, but it averages to zero during the longer period (Wilczak *et al.*, 2001).

Density fluctuation

In addition to the problems of an imperfect turbulent field, uncertainties also arise because of instrument-related problem is caused by density fluctuations in the air. The infrared gas analyzers used for CO_2 measurements basically detect the molar density of CO_2 (moles per unit volume) instead of mixing ratio. The molar density is affected not only by the number of CO_2 molecules in the air sample but also by the density of that sample. The air density fluctuates due to variations in the temperature and in the humidity of the sample, and these variations induce an apparent mean vertical wind component (Webb *et al.*, 1980). However, if the humidity and temperature variation are measured, these density changes can be taken into account

in every 10-*Hz* observation, or as usually, the correction is applied on the 30-min average as a function of the concurrently-measured heat and humidity fluxes (Webb *et al.*, 1980).

Data acquisition and processing

Spike detection

Spikes are typically characterized as short duration, large amplitude fluctuations that can be caused by random electronic spikes in the monitoring or recording systems as might occur during precipitation when water can collect on the transducers of some sonic anemometers. Quality control should include the identification and removal of spikes. For example, correlated spikes in the temperature and vertical velocity from sonic anemometer can contaminate the calculated heat flux. Spike that do not influence the fluxes still affect the variances. When the number of spikes becomes large, the entire data period should be considered suspect and discarded (Foken *et al.*, 2004). Vickers and Mahrt (1997) developed a despiking routine to allow spike identification and removal. They considered electronic spikes to have a maximum width of 3 consecutive points in the time series and amplitude of several standard deviations away from the mean. This routine was similar to the work of (Højstrup, 1993). The method computes the mean and standard deviation for a series of moving window of length. The window moves one point at a time through the series. Any point in the window which is more than 3.5 standard deviations from the window mean is considered a spike. The point is replaced using linear interpolation between data points. When 4 or more consecutive points are detected, they are not considered spikes and are not replaced. The entire

process is repeated until no more spikes are detected. During the second pass, when the standard deviations may be smaller if spikes were replaced on the previous pass, the threshold for spike detection increases to 3.6 standard deviations and a like amount for each subsequent pass. The threshold of 3.5 standard deviations is limited spike events to 3 or fewer consecutive points (Vickers and Mahrt, 1997).

Planar fit method

When an eddy-covariance setup is erected one will try to orient the vertical axis of the anemometer with the true vertical direction. In practice there will always be a (minute) deviation from the vertical and a corresponding bias in the flux-estimates. To eliminate the bias from the fluxes one has to align the frame of reference with the vertical using a coordinate rotation. There are mainly three methods to determine the orientation of a sonic relative to a Cartesian coordinate system aligned along the mean wind: double rotation ($\overline{v} = 0$ and $\overline{w} = 0$, according to Kaimal and Finnigan (1994)), triple rotation ($\overline{w'v'} = 0$), and planar fit ($\overline{v} = 0$ and normally $\overline{w} \neq 0$, according to Wilczak *et al.* (2001). In low wind speed conditions the mean wind direction for averaging periods ill defined and the errors in the double rotation and triple rotation can be large. The planar fit uses long intervals to determine the angles and does not suffer from this problem. Following Wilczak *et al.* (2001), the planar fit method for determining the orientation of a sonic anemometer relative to a streamline coordinate. The plane of the new coordinate system is defined by the horizontal wind components placed parallel to the surface and the *u*-component aligned to streamlines of the flow. The orientation of the plane can be determined by a least squares fit of the wind data to Equation:

$$\overline{w_m} = b_0 + b_1\overline{u_m} + b_2\overline{v_m}\,, \tag{1.11}$$

where $\overline{w_m}$, $\overline{u_m}$, and $\overline{v_m}$ are components of the (30-min) mean velocity in the instrument coordinate system and b_0, b_1 and b_2 are regression coefficients. The regression coefficients are used to determine the rotation angle α about the *v*-axis, the roll angle β about the intermediate *u*-axis and the yaw angle γ about the new *z*-axis (Figure 1.3). As the topography is almost flat no dependency of the rotation angles on wind direction is given and the angles are generally small.

By multiplying the measured data (subscript $_m$) with the matrices given in Equation 1.13, the data are rotated into the new coordinate system (subscript $_{rot}$).

$$\begin{bmatrix} u_{rot} \\ v_{rot} \\ w_{rot} \end{bmatrix} = \mathbf{MCD} \begin{bmatrix} u_m \\ v_m \\ w_m \end{bmatrix}, \tag{1.12}$$

where

$$\mathbf{M} = \begin{bmatrix} \cos\gamma & -\sin\gamma & 0 \\ \sin\gamma & \cos\gamma & 0 \\ 0 & 0 & 1 \end{bmatrix}, \tag{1.13}$$

$$\mathbf{C} = \begin{bmatrix} 1 & 0 & 0 \\ 0 & \cos\beta & -\sin\beta \\ 0 & \sin\beta & \cos\beta \end{bmatrix}, \tag{1.14}$$

$$\mathbf{D} = \begin{bmatrix} \cos\alpha & 0 & \sin\alpha \\ 0 & 1 & 0 \\ -\sin\alpha & 0 & \cos\alpha \end{bmatrix}. \qquad (1.15)$$

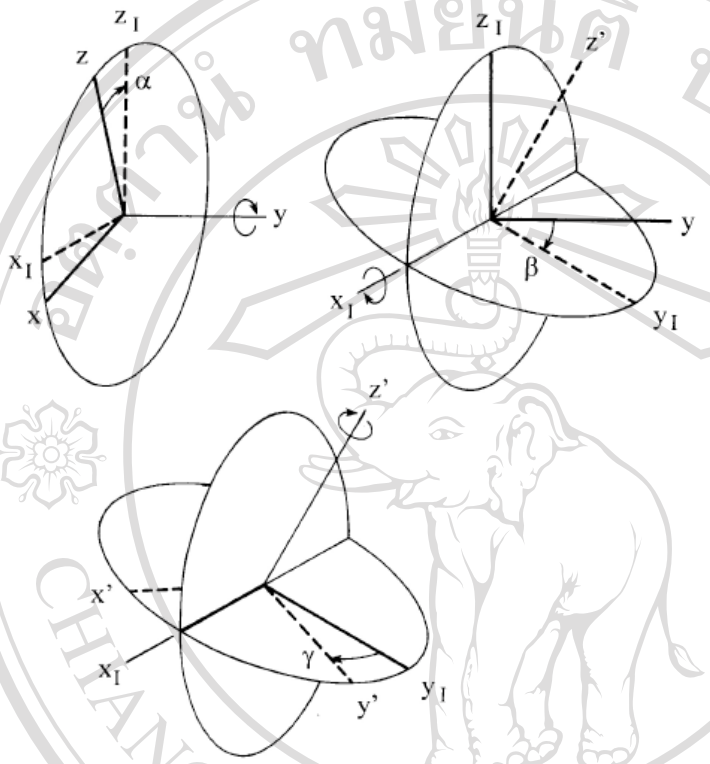

Figure 1.3 Definitions of the tilt angle α, β, and γ for the xyz convention. The original axes are x, y, and z, the intermediate axes are x_I, y_I, and z_I, and the final axes are x', y', and z' (from Wilczak *et al.*, 2001).

Linear detrending

Detrending operation used to separate the turbulent signals that are to be included in the eddy flux from trends or low frequency components imposed either by instrumental drift or as a result of changes in meteorological conditions. Over a suitable time interval the trend can be approximated as linear and the fluctuations with respect to the regression line can be obtained by linear detrending. In covariance

calculations the fluctuations are obtained by subtracting a signal from a realization mean $\bar{x}$, or in the case of detrending/filtering from an instantaneous mean X_t, $x_t' = x_t - X_t$, where $x = w, c$.

In linear detranding, the mean is given by the linear ligression line $X_t = St + I$ over the period T (= $N_i \Delta t$), the regression slope S and intercept I be determined by:

$$S = \frac{N_i \Sigma t x_t - \Sigma t \Sigma x_t}{N_i \Sigma t^2 - (\Sigma t)^2}, \tag{1.16}$$

$$I = \frac{\Sigma x_t - S \Sigma t}{N_i}, \tag{1.17}$$

where $t = i\Delta t$ and the summation is made over $i = 1, \ldots, N_i$ (Rannik and Vesala, 1999).

Corrections for changes in air density

A paper by Webb *et al.* (1980) drew attention to the need to consider corrections to the measured flux because of changes to air density. The simultaneous transfer of sensible and latent heat causes fluctuations in air density that can be erroneously attributed to fluctuations in CO_2 and latent heat in sensors that measure the partial density of CO_2 or H_2O in air. In general the correct flux of a scalar quantity is calculated after:

$$F_c = \overline{w'\rho_c'} + \mu \frac{\bar{\rho}_c}{\bar{\rho}_a} \overline{w'\rho_v'} + (1 + \mu\sigma)\bar{\rho}_c \frac{\overline{w'T'}}{\bar{T}}, \tag{1.18}$$

where μ is the ratio of molecular weights of dry air and water vapor, σ is the ratio of water vapor (ρ_v) and dry air (ρ_a)densities, and ρ_c is the CO_2 density measured by the open path CO_2/H_2O gas analyzer.

Simplified version of formula (Equation 1.18) for the flux of water vapor

$$\lambda E = \lambda(1+\mu\sigma)\left(\overline{w'\rho_v'} + \overline{\rho}_v \frac{\overline{w'T'}}{\overline{T}}\right). \qquad (1.19)$$

Soil CO_2 efflux or Soil respiration

As mentioned above, atmospheric CO_2 concentrations have been increasing in response to the disruption of the global carbon cycle by anthropogenic activities such as deforestation, agricultural practices and burning of fossil fuels. This has resulted in large shifts among terrestrial carbon pools, particularly soils (Rustad *et al.*, 2000). The world's soils contain an estimated 1550 Gt C (Jacobson *et al.*, 2000). This is hold about three times as much carbon as the terrestrial biosphere and about twice as much as the atmosphere. Scientists working on global warming and climate change have recently focused attention on soil as a major source and sink for atmosphere CO_2. The efflux of CO_2 from soil results from the combined rates of autotrophic (root) and heterotrophic (microbial and soil fauna) respiration; it is often call "soil respiration". Globally, soil respiration comprises a release of carbon to the atmosphere of about 75-80 Gt C per year (Raich *et al.*, 2002), which is nearly half of the gross primary productivity (*GPP*) of terrestrial ecosystems and about 10% of the total atmospheric carbon.

Controlling factors

Several reviews have examined the analysis and description of temperature-induced increases in soil respiration, and this relationship has been described using linear, power, sigmoid, and exponential equations (Janssens *et al.*, 2003). However, exponential relationships, especially Q_{10} relationships, are more frequently used to describe respiration rates from temperature. Soil moisture is another important factor influencing soil respiration. The relationship with soil moisture is more complex and depends on site-specific soil parameters (Howard and Howard, 1993). Soil moisture affects soil respiration by its direct influence on root and microbial activities, or indirect influence on soil physical and chemical properties. As soil moisture increases, respiration generally increases, but soil moisture may negatively affect respiration rates when it becomes either very high or too low. Low soil moisture may lead to lower quantities of dissolved organic carbon, which is an important substrate for heterotrophic soil respiration (Billings *et al.*, 1998). In very high soil moisture conditions, respiration rates are reduced due to inhibition of diffusivity within waterlogged soils and decreased oxygen availability. This relationship is sometimes described using a quadratic equation (Mielnick and Dugas, 2000). Other equations are also used to describe the influence of soil moisture on respiration: linear (Epron *et al.*, 1999); exponential (Davidson *et al.*, 1998; Fang and Moncrieff, 1999); and hyperbolic (Hanson *et al.*, 1993). Despite this, the relationship between soil respiration and moisture is usually scattered, and the understanding of this relationship the mechanisms underlying the relationship is still limited, compared to that of respiration and temperature relationship.

In addition to soil temperature and soil water content, other biotic and abiotic factors have been reported to influence soil CO_2 efflux such as soil organic matter quantity and quality (Cleveland *et al.*, 2006; Schlesinger and Andrews, 2000; Taylor *et al.*, 1989), root and microbial biomass (Han et al., 2007; Parkin et al., 2005; Vargas and Allen, 2008; Wang et al., 2003), and soil texture (Dilustro *et al.*, 2005; Raich and Potter, 1995; Wang *et al.*, 2003). In the presence of a drought, the amount and distribution of precipitation has also been shown to be an important controlling factor of soil CO_2 efflux (Cable and Huxman, 2004; Cable *et al.*, 2008; Chen *et al.*, 2008; Curiel Yuste *et al.*, 2003; Jarvis *et al.*, 2007; Lee *et al.*, 2002; Patrick *et al.*, 2007). Rain exerts control during dry periods either by controlling soil water content fluctuations in surface layers where most of the biological activity occurs (Lee *et al.*, 2002) or by strong stimulating soil CO_2 emissions in what called the "Birch effect" or "drying and rewetting effect" (Birch, 1958; Birch, 1959; Borken et al., 2003; Borken et al., 1999; Davidson et al., 2000; Jarvis et al., 2007; Lee et al., 2002). Rewetting of extremely dry soil usually causes a strong increase in CO_2 emissions, possibly because (1) a considerable proportion of soil microorganisms die during the drought (van Gestel *et al.*, 1991), leading to quick decomposition of dead cells; (2) the availability of organic substrates increases through desorption from the soil matrix (Seneviratne and Wild, 1985); and (3) the exposure of organic surfaces to microorganisms increases (Birch, 1959). Although pulses of CO_2 production following wetting of dry soils have been recognized for many years (e.g. Birch, 1958; Borken *et al.*, 2003; Fierer and Schimel, 2003; Liu *et al.*, 2002), there has been a paucity of studies elucidating how soil respiration responds to precipitation events, especially in agricultural soils. In the future, many regions of the globe may

experience higher mean annual temperatures and greater intra-annual variation in timing of precipitation events (IPCC, 2007). Under these scenarios, we would expect many surface soils to experience more frequent drying and rewetting events (IPCC, 2007). Therefore, the study of soil CO_2 released from soils following precipitation is critically important in shaping our understanding the implications of climate change on soil carbon sequestration.

Methods of measurements and estimations

Soil respiration or soil CO_2 efflux has been extensively measured using various methods. An early method, soil air was collected periodically by suction through gas sampling tubes buried at various depths, and then the small air samples were manually analyzer for soil CO_2 concentration with an infrared gas analyzer (IRGA), gas chromatograph or gas detection tube to study CO_2 profile and diffusion (Davidson and Trumbore, 1995). The gas extraction method can provide information on soil CO_2 production at several depths, but it can not provide *in situ*, continuous and convenient data on CO_2 efflux. Furthermore, this method will disturb the soil environment. An unavoidable bias may occur during the processes of gas extraction, storage, transport, and measurement.

In addition to the gas extraction method, measurements to determine soil CO_2 efflux are often made with the different chamber techniques where a bottomless chamber is mounted tightly on top of the ground and the CO_2 concentration within the chamber is recorded in order to find out the amount of CO_2 emitted from the soil. The three major chamber techniques used widely for measuring soil gas fluxes are closed static chamber, closed dynamic chamber and open dynamic chamber. Closed static

chamber techniques are based either on enrichment or absorption of CO_2 in the headspace. The alkali solution method (Lundegårdh, 1927) is probably the oldest method, while the soda lime method (Biscoe *et al.*, 1975) is probably the most frequently used technique because it is inexpensive, easy to use, and particularly suitable where spatial variation is large (Keith *et al.*, 1997).In closed dynamic chamber IRGA systems, air circulates in a loop between the chamber and an external IRGA, and the change in CO_2 concentration over time is measured (Goulden and Crill, 1997). In open dynamic chamber systems have a constant airflow through the chamber, and the difference in CO_2 concentrations of the ambient and internal air at the inlet and the outlet are continuously monitored (Fang and Moncrieff, 1996). The chambers always disturb the system being measured, each chamber type having its own advantages and disadvantages. Among the primary disadvantages of soil chamber measurements are the lack of continuous observations, manual setup, and disturb soil surface boundary conditions that could alter the nature of the diffusive flux (Davidson *et al.*, 2002). Attempts to improve temporal coverage by continuous air pumping from the enclosure to a gas analyzer resulted in significant alteration of the soil-atmosphere boundary conditions due to variations in air pressures with in the chamber (Lund *et al.*, 1999) and perturbation of natural conditions on the soil surface, such as effecting the local vegetation, the wind and the precipitation. In recent years, researchers developed automated surface chamber measurements capable of capturing short-term changes in soil respiration. However, these quasi-continuous systems are still limited to soil CO_2 effluxes lacking details regarding subsurface CO_2 dynamics.

The recently developing soil CO_2 vertical gradient measurement method provides an opportunity to measure soil respiration with the high frequency with the

minimum disturbance to natural structure of the soil. In this method, the CO_2 concentration inside the soil pores is measured at a number of depths from the soil surface with carbon dioxide measurement probes buried in the ground. The soil CO_2 efflux can be calculated by applying Fick's first law of diffusion:

$$F_z = -D_s \frac{dC}{dz}, \tag{1.20}$$

where F_z is the soil CO_2 efflux, D_s the gaseous CO_2 diffusion coefficient in the soil that varies with soil, C is the CO_2 mole concentration at a certain depth of the soil, and z the depth. For flux determination, the gradient is approximated by discrete differences ΔC and Δz.

Soil gaseous diffusion coefficient

Assessment of soil gas diffusivity is done in different ways that are more complementary than exclusive: theoretical, based on physical laws (Jaynes and Rogowski, 1983), modeling methods which combine empirical and physically based relationships (Moldrup *et al.*, 1996) and empirical approaches, based on *in situ* or laboratory measurements (Lai *et al.*, 1976). When considering gas diffusion coefficients in soil, a relative gas diffusion coefficient (D_s/D_a), i.e., the ratio of the gas diffusion coefficient in soil to that in free air, is usually used.

In general, the gas diffusion coefficient in free air is affected by temperature and pressure:

$$D_a = D_{a0}\left(\frac{T}{T_0}\right)^{1.75}\left(\frac{P}{P_0}\right), \qquad (1.21)$$

where T is the temperature (K), P the air pressure (Pa), D_{a0} a reference value of D_a at T_0 (20 °C or 293.15 K) and P_0 (1.013 x 10^5 Pa), and is given as 1.47 x 10^{-5} m^2 s^{-1} (Jones, 1992).

The relative gas diffusion coefficient (D_s/D_a) has been defined as the gas tortuosity factor, ξ (Jury *et al.*, 1991). There are several empirical models for computing ξ. Early ξ models depended only on the soil air-filled porosity (ε). Penman (1940) proposed a linear relationship between ξ and ε, while Marshall (1959) and Millington (1959) found that ξ was given by $\varepsilon^{3/2}$ and $\varepsilon^{4/3}$, respectively. The most widely used of these one-parameter models is the Penman (1940) model:

$$\xi = 0.66\varepsilon . \qquad (1.22)$$

The next generation of ξ models also included in soil-type effects in the form of the soil total porosity, ϕ. The most widely used two-parameter model is that of Millington and Quirk (1961):

$$\xi = \frac{\varepsilon^{10/3}}{\phi^2}. \qquad (1.23)$$

Comparing gas diffusivity models with measured data for number of differently textured sieved and repacked soils, Jin and Jury (1996) concluded that the hitherto overlooked Millington and Quirk (1960) model:

$$\xi = \frac{\varepsilon^2}{\phi^{2/3}}, \tag{1.24}$$

best described the measured data as compared to the classical models. Moldrup *et al.* (1997) combined the Penman and Millington and Quirk model approaches into the general PMQ model:

$$\xi = 0.66\varepsilon\left(\frac{\varepsilon}{\phi}\right)^{\frac{12-m}{3}}, \tag{1.25}$$

and showed that m = 3 for gas diffusivity in undisturbed soils, and m = 6 for gas diffusivity in sieved, repacked soils, gave improved descriptions compared to earlier two-parameter ξ models. This study also implied a significant difference between gas diffusivity in undisturbed and repacked soils and a larger soil-type dependency for gas diffusivity in undisturbed compared to repacked soil.

Werner *et al.* (2004) pointed to the following simple relationship proposed by Moldrup *et al.* (2004) as the best predictor of gaseous diffusion coefficient as a function of air-filled porosity not only for sieved and repacked soils but also for in situ measurements:

$$\xi = \frac{\varepsilon^{2.5}}{\phi}. \qquad (1.26)$$

Soil CO_2 gradient method

This method has not been widely used earlier probably due to instrument limitations and difficulty in calculating soil surface CO_2 efflux from gradient measurements and CO_2 diffusivity in the soil. The first disadvantage is currently eliminated or minimized with the technological improvements, and the latter one can be diminished by modeling methods. Recently, an innovative CO_2 sensor was developed for air quality monitoring and control. This instrument has potential to be buried in the soil and measure CO_2 in the soil atmosphere. Hirano *et al.* (2003) first used a type of these small CO_2 sensors (GMD20, Vaisala Inc., Finland) buried in the soil under a cool-temperate deciduous broadleaf forest in Japan to deduce soil respiration, and therefore have demonstrated the feasibility of the instrument. To develop more measurement method in soil CO_2 efflux, Tang *et al.* (2003) used the new small solid-state CO_2 sensors (GMT222, Vaisala Inc., Finland) to monitor continuously soil CO_2 profiles and soil CO_2 efflux in a dry season in a Mediterranean savanna ecosystem in California by burying these CO_2 sensors at different depths of the soil. Based on the measurement of the soil CO_2 gradient and the diffusion coefficient estimated from the Millington-Quirk model. They found that the estimated CO_2 efflux was very close to chamber measurements and can be used for long-term continuous measurements of soil CO_2 efflux. Liang *et al.* (2004) compared four approaches for measuring soil CO_2 efflux in a northern larch (*Larix kaempferi* Sarg.) forest. The four approaches for measuring soil CO_2 efflux were: (1) a widely used

non-steady-state LI-6400 chamber system (LI-COR, Lincoln, NE, USA); (2) a steady-state chamber system with 9 open-top chambers; (3) a steady-state chamber with 16 automated chambers; and (4) a soil CO_2 gradient system (GMT222, Vaisala Inc., Finland), the diffusion coefficient was measured in the laboratory as a function of water content by purging oxygen from a diffusion chamber and measuring the change in oxygen concentration with time. They found that soil CO_2 efflux measured with the soil CO_2 gradient approach was, on average, 45% higher than the results of the automated chamber approach, but the correlation between the two technique was good (R^2=0.77). Tang *et al.* (2005) used GMT222 continuously measured CO_2 concentration at various depths in soil and calculated soil CO_2 efflux based on CO_2 gradients and diffusivity in a young ponderosa pine plantation in the Sierra Nevada Mountains of California and used this method to understand the diurnal and seasonal variation in soil respiration. Furthermore, Jassal *et al.* (2005) used these sensors for long-term continuous real-time measurement of CO_2 concentrations at different depths, and measure half-hourly soil CO_2 effluxes with an automated non-steady-state chamber, to understand the biotic and abiotic factors that control soil CO_2 efflux, they compared seasonal and diurnal variations in simultaneously measured forest-floor CO_2 effluxes and soil CO_2 concentration profiles in a Douglas fir forest on the east coast of Vancouver Island. They found that soil CO_2 efflux that calculated from soil CO_2 concentration gradients near the surface closely agreed with the measured efflux and they also found that more than 75% of soil CO_2 efflux originated in the top 20 cm. soil. Turcu *et al.* (2005) tested the gradient method using under steady- and transient-state soil water content and temperature conditions and compared results with a surface chamber CO_2 flux system. The Vaisala GMD20 (Vaisala Inc., Woburn,

MA) sensors was installed in the soil profile providing continuous record of CO_2 concentration gradients coupled with concurrent estimates of water content-dependent gaseous diffusion coefficient enabling calculation of surface gaseous flux. They found that an imposed CO_2 concentration gradient in dry a soil column resulted in agreement with chamber-measured fluxes. A series of continuous concentration measurements under variable water content conditions and wetting events showed agreement with surface chamber measurements. Myklebust *et al.*(2008) compared measurements of soil CO_2 efflux using soil chambers and the soil CO_2 gradient method that was covered with living vegetation, straw, and snow in turn through a year. They found that the soil CO_2 gradient and soil chambers method agreed in the most conditions but neither was accurate in all conditions. Collar interference with snow and the effect of vegetation removal caused measurements to be inaccurate. Moreover, the study by Riveros-Iregui *et al.* (2008) at the subalpine forest of the northern Rocky Mountains found that agreement between the soil CO_2 gradient and soil chambers method was limited during high soil water content conditions and after summer rainfall.

The urgent need for determine continuous soil CO_2 efflux and associated concentration profiles for extended period is widely recognized as a key to reliable integration of total CO_2 exchange between soil and the atmosphere (Parkin and Kaspar, 2004).